Biogeosciences Discuss., https://doi.org/10.5194/bg-2019-144
Manuscript under review for journal Biogeosciences
Discussion started: 6 May 2019
© Author(s) 2019. CC BY 4.0 License.

Microbial community composition and abundance after millennia of submarine permafrost warming

Julia Mitzscherling[1], Fabian Horn[1], Maria Winterfeld[2], Linda Mahler[1], Jens Kallmeyer[1], Pier P. Overduin[3], Lutz Schirrmeister[3], Matthias Winkel[4], Mikhail N. Grigoriev[5], Dirk Wagner[1,6] and Susanne Liebner[1,7]

[1]GFZ German Research Centre for Geosciences, Helmholtz Centre Potsdam, Section 3.7 Geomicrobiology, 14473 Potsdam, Germany
[2]Alfred Wegener Institute, Helmholtz Centre for Polar and Marine Research, Marine Geochemistry, 27570 Bremerhaven, Germany
[3]Alfred Wegener Institute, Helmholtz Centre for Polar and Marine Research, Permafrost Research, 14473 Potsdam, Germany
[4]GFZ German Research Centre for Geosciences, Helmholtz Centre Potsdam, Section 3.5 Interface Geochemistry, 14473 Potsdam, Germany
[5]Siberian Branch, Russian Academy of Sciences, Mel'nikov Permafrost Institute, Yakutsk, Russia
[6]University of Potsdam, Institute of Geosciences, 14476 Potsdam, Germany
[7]University of Potsdam, Institute of Biochemistry and Biology, 14476 Potsdam, Germany

Correspondence to: Susanne Liebner (Susanne.Liebner@gfz-potsdam.de)

Abstract. Warming of the Arctic led to an increase of permafrost temperatures by about 0.3°C during the last decade. Permafrost warming is associated with increasing sediment water content, permeability and diffusivity and could on the long-term alter microbial community composition and abundance even before permafrost thaws. We studied the long-term effect (up to 2500 years) of submarine permafrost warming on microbial communities along an onshore-offshore transect on the Siberian Arctic Shelf displaying a natural temperature gradient of more than 10 °C. We analysed the in-situ development of bacterial abundance and community composition through total cell counts (TCC), quantitative PCR of bacterial gene abundance and amplicon sequencing, and correlated the microbial community data with temperature, pore water chemistry and sediment physicochemical parameters. On time-scales of centuries, permafrost warming coincided with an overall decreasing microbial abundance while millennia after warming microbial abundance was similar to cold onshore permafrost and DOC content was least. Based on correlation analysis TCC unlike bacterial gene abundance showed a significant rank-based negative correlation with increasing temperature while both TCC and bacterial gene copy numbers showed a negative correlation with salinity. Bacterial community composition correlated only weakly with temperature but strongly with pore-water stable isotope signatures and depth. Microbial community composition showed substantial spatial variation and an overall dominance of Actinobacteria, Chloroflexi, Firmicutes, Gemmatimonadetes and Proteobacteria which are amongst the microbial taxa that were also found to be active in other frozen permafrost environments. We suggest that, millennia after

permafrost warming by over 10°C, microbial community composition and abundance show some indications for proliferation but mainly reflect the sedimentation history and paleo-environment and not a direct effect through warming.

1 Introduction

Temperatures in high-latitude regions have been rising twice as fast as the global average over the last 30 years (IPCC in Climate Change 2013, 2013) and are predicted to experience the globally strongest increase in the future (IPCC in Climate Change 2013, 2013; Kattsov et al., 2005). In the northern hemisphere, 24 % of the land surface (Zhang et al., 2003) and large areas of the Arctic shelves are underlain by permafrost (Brown et al., 1997). With 1672 Pg carbon (Schuur et al., 2008), the northern circumpolar permafrost zone stores about twice as much carbon as currently found in the atmosphere (Schuur et al., 2009; Zimov et al., 2006). About 88% of this carbon occurs in permafrost soils and deposits (Tarnocai et al., 2009). Permafrost harbours numerous ancient but viable cells (Bischoff et al., 2013; Gilichinsky et al., 2008; Graham et al., 2012; Koch et al., 2009; Mackelprang et al., 2011; Wagner et al., 2007) that can remain active at extremely low temperatures (Hultman et al., 2015; Rivkina et al., 2000). With increasing permafrost age, microbial communities show adaptations to the permafrost biophysical environment and specialize towards long-term survival strategies such as increased dormancy, DNA repair or stress response (Johnson et al., 2007; Mackelprang et al., 2017). Following the trend of air temperature increase in the northern hemisphere, continuous permafrost warmed by about 0.3°C over the last decade at a global scale (Biskaborn et al., 2019). Warming of permafrost can substantially increase liquid water content, sediment diffusivity and permeability (Overduin et al., 2008; Rivkina et al., 2000; Watanabe and Mizoguchi, 2002) potentially mobilizing carbon in the form of trapped methane (Portnov et al., 2013; Shakhova et al., 2010, 2014; Thornton et al., 2016). Microbial community composition was reported to be responsive to temperature changes (Luo et al., 2014; Rui et al., 2015; Weedon et al., 2012; Xu et al., 2015; Zhang et al., 2005; Zogg et al., 1997). However, results on the extent of these community changes and their dependence on exposure time are contradictory (Allison et al., 2010; Schindlbacher et al., 2011; Walker et al., 2018; Weedon et al., 2017; Xiong et al., 2014; Zhang et al., 2016). In general, the microbial community response to warming appears to be delayed (DeAngelis et al., 2015) and the effect of warming might take decades to affect the microbial community composition (Radujković et al., 2018; Rinnan et al., 2007). Not only microbial community composition can be responsive to temperature but also microbial abundance especially in systems with weak energy constraints. Microbial abundance correlates with enzymatic activities and methane production (Taylor et al., 2002; Waldrop et al., 2010), which are sensitive to temperature. Microbial growth, respiration and carbon uptake can correlate with microbial biomass (Walker et al., 2018). Thus, substantial permafrost warming on long time-scales could affect microbial community composition and abundance before permafrost thaws.

Submarine permafrost provides an analogue for rising permafrost temperatures over time-scales of centuries and millennia. Submarine permafrost of the Arctic Sea shelves originally formed under terrestrial (subaerial) conditions and was inundated

© Author(s) 2019. CC BY 4.0 License.

by post-glacial sea level rise during the Holocene (Romanovskii and Hubberten, 2001). Upon sea transgression, permafrost degraded over thousands of years as the relatively warm ocean water warmed the submerged sea floor. Mean annual bottom water temperatures in the Laptev Sea (East Siberian Arctic shelf) are 12 to 17 °C warmer than the annual average surface temperature of terrestrial permafrost (Romanovskii et al., 2005). Even today, new submarine permafrost is created by erosion of Arctic permafrost coasts (Fritz et al., 2017), which account for 34% of the coasts worldwide (Lantuit et al., 2012). In a recent study, we compared submarine sediment cores from two locations on the Siberian Arctic Shelf and looked at the combined effect of permafrost inundation time and seawater intrusion on microbial communities. We showed that flooding by sea water reduced permafrost bacterial abundance and changed bacterial community composition due to the penetration of seawater into a former freshwater habitat (Mitzscherling et al., 2017). It was suggested that in addition to the effect of seawater infiltration, the sediment warming taking place over millennia could lead to proliferation. However, the specific effect of long-term permafrost warming independent of thawing has not been assessed so far. Here we hypothesize that millennial-scale permafrost warming directly increases microbial abundance and alters microbial community composition. We used submarine permafrost sediments of comparable age and physicochemical properties that differed in temperature by more than 10 °C due to different periods of inundation and sediment warming and assessed total microbial and bacterial abundances and community composition relative to temperature, pore-water chemistry and sedimentation history.

2 Materials and Methods

2.1 Study site and drilling

The study area (~73°60'N, 117°18'E) is situated in the western part of the Laptev Sea, on the East Siberian Arctic Shelf (Fig. 1). Mean annual bottom water temperatures in the Laptev Sea range between -1.8 °C to -1 °C (Wegner et al., 2005) leading to sediment temperatures of -1.0 °C and -2.0 °C within the largest part of the shelf (Romanovskii et al., 2004). We investigated four cores (C1-C4, Fig. 2a) that were retrieved along an onshore-offshore transect in the coastal region of Cape Mamontov Klyk in 2005 (Overduin, 2007; Rachold et al., 2007). Drilling was performed with a hydraulic rotary-pressure mechanism (URB-2A-2) and without utilizing of drill fluid. All samples were frozen immediately after recovery and were kept at -22 °C until further processing. Cores were named after the order of drilling and we kept this order (C1, C4, C3, C2) for better comparability with previous studies (Koch et al., 2009; Mitzscherling et al., 2017; Overduin et al., 2008; Winkel et al., 2018).

Assuming a constant mean annual coastal erosion rate of 4.5 m yr^{-1} (Grigoriev, 2008) the drill site located furthest offshore (C2, 11.5 km off the coast) was inundated approximately 2500 years ago (Rachold et al., 2007). Accordingly, the drill sites C3 and C4, located 3 km and 1 km off the coast, were inundated around 660 and 220 years ago, respectively. More recent analysis based on remote sensing shows that 40-year coastal erosion rates for the same stretch of coastline between 1965 and 2007 were slower (about 2.9 m yr^{-1}) (Günther et al., 2013), which would translate into even longer inundation periods.

© Author(s) 2019. CC BY 4.0 License.

However, in the present study we refer to Grigoriev (2008), which are based on direct observations of coastal erosion at the C1 coring site. From onshore to offshore all cores were characterized by an increase in water depth, in depth to the ice-bonded permafrost table (Fig. 2a, Table S1) and in ground temperature (Table S2) (Overduin, 2007; Rachold et al., 2007). Temperature measurements at all sites were done using thermistors and infra-red sensors (Junker et al., 2008).

2.2 Sample selection

Each of the four drill cores exhibited different sedimentological units. Lithostratigraphic Unit II was identified in all cores (Fig. 2a) and was entirely located within the ice-bonded permafrost. Depth location of Unit II within each core can be found in Table S1. This unit was deposited during the late Pleistocene, was warmed without thawing, and had so far remained unaffected of seawater infiltration. On the basis of a PCA analysis (see next chapter and Fig. 3) and previous lithostratigraphic descriptions (Winterfeld et al. 2011) all further analysis was conducted on samples from Unit II. The ages of the sediment are published in Winterfeld et al. (2011). The present study refers to sediment ages determined by optically stimulated luminescence (OSL) on quartz and infrared optically stimulated luminescence (IR-OSL) on feldspars. OSL ages of Unit II sediments from core C1 range from 30.5 ± 2.0 ka at 22 m below surface (m bs) to 114 ± 6 ka at 50 m bs. OSL ages range from 97 ± 6 to 112 ± 8 ka between 23 and 30 m below sea floor (m bsf) in core C3 and from 133 ± 8 to 148 ± 14 ka between 37 and 53 m bsf, and increase with depth. IR-OSL ages date back to 59 ± 5.8 ka at around 15 m bsf in C4 and 86 ± 5.9 ka at 44 m bsf and 111 ± 7.5 ka at 77 m bsf in C2. Consequently, sediments of Unit II were deposited during the early to middle Weichselian (Winterfeld et al., 2011).

For molecular analyses we took 6 replicate samples from each of the cores C1 (C1-1 – C1-6), C4 (C4-1 – C4-6) and C3 (C3-1 – C3-6) and 8 replicates from core C2 (C2-1, C2-2, C2-4, C2-5, C2-7, C2-8, C2-9, C2-10) (Fig. 2a). Those replicates were located at different depths within Unit II (Table S4). The unit was mainly composed of sands with varying proportions of silt and to a minor extent of clay, and a frequent occurrence of wood fragments, plant detritus interlayers and small peat inclusions (Winterfeld et al., 2011). Both, sandy as well as organic-rich deposits were represented by three replicates in C1, C4 and C3 and four replicates in C2 (Table S4). Furthermore, to check for reproducibility we included samples from C2 retrieved in a previous study (Mitzscherling et al., 2017) (sample names CK12xx). To minimize contamination we took the subsamples from the centre of the core.

2.3 Pore water and sediment analyses

Pore water of segregated ground ice was extracted from thawed subsamples of the sediment cores using rinsed Rhizons™ (0.15 µm pore diameter). Electrical conductivity, salinity, cation and anion concentrations, stable isotope concentrations ($\delta^{18}O$, δD), and pH were measured for 183 samples of C1, 67 samples of C2, 38 samples of C3 and 10 samples of C4 in Unit II (Table S3). Electrical conductivity, salinity and pH were measured with a WTW MultiLab 540 using a TetraConTM 325 cell referenced to 20°C. Total dissolved element concentrations (Ba^{2+}, Ca^{2+}, K^{+}, Mg^{2+}, Na+, Si_{aq}) were determined by

© Author(s) 2019. CC BY 4.0 License.

inductively coupled plasma optical emission spectrometry (ICP-OES, Optima 3000XL, Perkin-Elmer, Waltham) (Boss and Frieden, 1989). Dissolved anion concentrations (Cl^-, SO_4^{2-}, Br^-, NO_3^-) were measured using a KOH eluent and a latex particle separation column on a Dionex DX-320 ion chromatographer (Weiss, 2001). The stable water isotopes (δD and$\delta^{18}O$) of segregated ground ice were determined following (Meyer et al., 2000) using a Finnigan MAT Delta-S mass spectrometer in combination with two equilibration units (MS Analysetechnik, Berlin).

Dissolved organic carbon (DOC) was measured as non-purgeable organic carbon via catalytic combustion at 680 °C using a Shimadzu TOC-VCPH instrument on samples treated with 20 µl of 30% supra-pure hydrochloric acid. The ice content was determined gravimetrically. Grain sizes were measured with a Coulter LS 200 laser particle size analyzer. The total organic carbon (TOC) was measured with the element analyser VARIO MAX C, while total carbon (TC), total nitrogen (TN) and total sulfur (TS) contents were determined with a CNS analyzer (Elementar Vario EL III).

2.4 DNA extraction

Core subsamples were homogenized in liquid nitrogen and DNA was extracted from ~5 g of sediment using a modified protocol of Zhou et al. (1996). The method was described before (Mitzscherling et al., 2017) and in the following we refer to these samples as molecular samples. Quality of the extracted genomic DNA was assessed via gel electrophoresis. DNA concentration was quantified with the Qubit2 system (Invitrogen, HS-quant DNA) and the crude DNA was purified using the HiYield PCR Clean-Up & Gel-Extraction Kit (SLG) to reduce PCR inhibitors prior to PCR applications.

2.5 Quantification of the bacterial 16S rRNA gene

Quantitative PCR was performed using the CFX Connect™ Real-Time PCR Detection System (Bio-Rad Laboratories, Inc.) and the primers S-D-Bact-0341-b-S-17 and S-D-Bact-0517-a-A-18 for the bacterial 16S rRNA gene (Table S5). Each reaction (20 µl) contained 2x concentrate of iTaq™ Universal SYBR® Green Supermix (Bio-Rad Laboratories), 0.5 µM of each the forward and reverse primer, sterile water and 2 µl of template DNA. The qPCR assays comprised the following steps: initial denaturation for 3 min at 95 °C, followed by 40 cycles of denaturation for 3 sec at 95 °C, annealing for 20 sec at 58.5 °C, elongation for 30 sec at 72 °C and a plate read step at 80 °C for 0.3 sec. Melt curve analysis from 65-95 °C with 0.5°C temperature increment per 0.5 sec cycle was conducted at the end of each run. The qPCR assay was calibrated using known amounts of PCR amplified gene fragments from a pure *Escherichia coli* culture. For each sample three technical replicates were analysed and DNA templates were diluted 5- to 100-fold prior to qPCR analysis. The PCR efficiencies based on standard curves were calculated using the BioRad CFX Manager software. They varied between 93 and 99%. All cycle data were collected using the single threshold Cq determination mode.

Biogeosciences Discuss., https://doi.org/10.5194/bg-2019-144
Manuscript under review for journal Biogeosciences
Discussion started: 6 May 2019
© Author(s) 2019. CC BY 4.0 License.

2.6 High throughput Illumina16S rRNA gene sequencing and analysis

Sequencing of each sample was performed in two technical replicates. Primers comprised different combinations of barcodes (Table S6). PCR amplification was carried out with a T100™ Thermal Cycler (Bio-Rad Laboratories, CA, USA). The PCR mixtures (25 µl) contained 1.25 U of OptiTaq DNA Polymerase (Roboklon), 10x concentrate buffer C (Roboklon), 0.5 µM of the sequencing primers S-D-Bact-0341-b-S-17 and S-D-Bact-0785-a-A-21 (Table S5), dNTP mix (0.2 mM each), additional 0.5 mM of $MgCl_2$ (Roboklon), PCR-grade water, and 2.5 µl of template DNA. Thermocycler conditions as well as clean up and quantification of PCR products, library preparation, Illumina MiSeq sequencing (GATC, Germany) and raw sequence data analysis were performed as described before (Mitzscherling et al., 2017). The number of PCR cycles was chosen to be 35. OTUs were taxonomically assigned employing the SILVA database (release 123) with a cutoff value of 97%.

2.7 Total cell counts

Preparation and quantification of the total cell abundance per g sediment were performed after (Llobet-Brossa et al., 1998). The modified protocol was described before by Mitzscherling et al. (2017). Briefly, cells were fixed with 4% paraformaldehyde in phosphate-buffered saline (PBS). After incubation, the sediment was pelleted by centrifugation for 5 min at 9600 g and washed in sterile filtered PBS. Two subsamples of each sample were diluted in PBS and filtered onto a polycarbonate membrane filter (0.2 µm) by applying a vacuum. Total cell counts were determined by SYBR Green I. Fluorescence microscopy was performed with a Leica DM2000 fluorescence microscope using the FI/RH filter cube. A magnification of 100x was used to count cells of either 200 fields of view or until 1000 cells were counted. We counted two filters per sample.

2.8 Statistics

Prior to statistical analysis, absolute singletons and $OTU_{0.03}$ (operational taxonomic units of clustered sequences with 97% similarity level) not classified as bacteria or classified as chloroplasts or mitochondria were removed. In addition, $OTU_{0.03}$ with reads <0.5% of total read counts in each sample were removed to reduce background noise. The background noise was estimated with the help of a positive control (*E. coli*), where the number of OTUs is known prior to sequencing. Absolute read counts were transformed into relative abundances in order to standardize the data and to make technical replicates comparable. Relative abundances of technical replicates were merged to mean relative abundances for bacterial community analysis i.e. the bubble plot and CCA. Samples having < 15.000 raw reads were checked for divergent relative abundances within duplicates (Table S7) and excluded from the calculation of mean relative abundances when the discrepancy was too big. Variation in $OTU_{0.03}$ composition, 16S rRNA gene and total cell abundance between samples and among drill sites, as well as correlations of the abundance and $OTU_{0.03}$ composition with environmental parameters were assessed using the Past

© Author(s) 2019. CC BY 4.0 License.

3.14 software (Hammer et al., 2001). Principal component analyses (PCA) based on Euclidean distance were used to assess variation in environmental variables across the different sediment units and within Unit II. Prior to analysis, all environmental data were standardized by subtracting the mean and dividing by standard deviation. To assess the correlations of bacterial and microbial abundance with environmental parameters the rank-based Spearman correlation was calculated. Mantel tests were used to study the relationship between environmental parameters and bacterial community composition (Mantel, 1967). A canonical correspondence analysis (CCA) was conducted to visualize the dependence of the bacterial communities on environmental parameters. PerMANOVAs were conducted (Anderson, 2001) to test whether communities or abundances were significantly different between drill sites. Analysis of variance (ANOVA) and the Dunn's post-hoc test were conducted to test whether DOC concentrations of the cores differed.

3 Results

3.1 Physicochemical pore water and sediment properties

Temperature (Fig. 2b) of Unit II was lowest in the terrestrial borehole (C1, constantly at around -12.4 °C at the time of drilling (Junker et al., 2008) and between -12.0 and -12.5 °C recently measured over a 2 year period (Kneier et al., 2018)) and increased with distance to the shore. According to (Junker et al., 2008) C4 exhibited a temperature range from -7.1 to -5.8 °C. Ground temperatures of C3 and C2 were similar with mean values of -1.4 and -1.5 °C, respectively, and showed marginal variation. C3 exhibited a slightly higher mean temperature than the longest inundated core C2.

Overall, the salinity of Unit II was low (Fig. 2b, (Winterfeld et al., 2011)). In C4, the drill site located closest to the coast, Unit II had the highest pore water salinity (mean = 5.6 PSU) ranging from 0.9 to 17.6 PSU (Table S2), which spans freshwater to mesohaline water but is much below seawater salinities. Salinity in C3 reached a mean value of 1.1 PSU. The submarine core furthest offshore (C2) and the terrestrial core (C1) had a mean pore water salinity of around 0.8 and 0.5 PSU, respectively. The stable water isotopes δD and $\delta^{18}O$ of the sediment cores C1 and C4 exhibited similar mean values of -22 ‰ for $\delta^{18}O$ and around -178 ‰ for δD, albeit a greater variance in C1 (Fig. 2c, Table S2). Sediments of C3 were characterized by higher and constant isotope values of around -20 ‰ for $\delta^{18}O$ and -158 ‰ for δD. In core C2, the isotope values were smaller with mean values of -28 ‰ for $\delta^{18}O$ and -213 ‰ for δD (Table S2).

DOC concentrations were lowest in Unit II of core C2, the core furthest offshore, and ranged from 4 to 41 mg C L^{-1}, with a mean value of 17 mg C L^{-1} (Fig. S1). Towards the coast the DOC content increased to mean values of 43 mg C L^{-1} in C3 and 96 mg C L^{-1} in C4. The terrestrial core C1 had a mean DOC concentration of around 48 mg C L^{-1} with values ranging from 4 to 305 mg C L^{-1}, thereby having by far the highest measured DOC concentration of all cores. The TOC content in this Unit II was generally very low with mostly < 0.5 wt%. While C1 and C4 had lowest mean values of 0.17 wt%, the TOC content increased with distance to the coast to 0.22 wt% in C3 and 0.33 wt% in C2 (Table S4). The pH of Unit II sediments ranged from slightly acidic to slightly alkaline values. In cores C1 and C4 the pH ranged from 5 to 7.9, whereas values of C2 and C3

© Author(s) 2019. CC BY 4.0 License.

were higher ranging from pH 6.5 to 8.0. Mean pH values of all cores were around pH 7 to 7.5. Other pore water data like anion and cation concentrations, conductivity, CNS, grain sizes and the gravimetrically determined water content can be found in Table S3.

All environmental, sedimentological and pore water data (Table S3) were used to conduct principal component analyses (PCA) to check for the level of similarity within Unit II. Unit II formed a dense cluster relative to the other sediment units (Fig. 3 Insert). Focusing on samples from Unit II only (Fig. 3) confirmed highly similar physicochemical characteristics of this unit in all cores even though C2 and C3 clustered along the axis PC2, while C1 and C4 were more randomly scattered. Variance between samples was mainly explained by grain sizes, stable water isotope concentrations and to a lesser extent by pH.

3.2 Microbial abundance

Overall microbial abundance decreased from onshore to offshore (C1, C4, C3) and had increased again in the drill site located furthest from the coast (C2). The terrestrial permafrost core C1 and the submarine core C2 had highest DNA concentrations (Fig. S2), total cell counts (TCC) (Fig. 4a) and bacterial 16S rRNA gene copy numbers of all cores (Fig. 4b). Lowest DNA concentrations and TCC were observed in core C3, whereas lowest numbers of bacterial 16S rRNA gene copies were found in core C4. All three abundance measures (DNA concentrations, TCC, and bacterial 16S rRNA gene copy numbers) significantly correlated with each other (Table S8). DNA concentrations reached mean values of 141.6 ng g^{-1} and 106.9 ng g^{-1} in C1 and C2, respectively, whereas the mean DNA concentration in C4 and C3 were 88.5 and 19.8 ng g^{-1} (Table S9). Mean TCC reached a value of 5 x 10^7 g^{-1} in C1. C4 and C2 had similar values of 1.3 x 10^7 g^{-1} and 1.5 x 10^7 g^{-1}, while cell numbers of C3 were one order of magnitude lower (1.5 x 10^6 g^{-1}). Bacterial 16S rRNA gene copy numbers usually exceeded TCC by an order of magnitude, with mean values of 1.6 x 10^8 g^{-1} and 2.9 x 10^8 g^{-1} in C1 and C2, but lower mean values of 3.6 x 10^7 g^{-1} and 1.7 x 10^7 g^{-1} in C4 and C3, respectively.

A correlation analysis (Table 1) revealed that microbial and bacterial abundance including DNA concentrations, 16S rRNA bacterial gene copies and TCC showed a significant rank-based negative correlation with salinity ($p < 0.05$, Spearman $-0.63 \leq r_s \leq -0.35$), cations ($K^+$, Mg^{2+}, Na^+) and anions (Cl^-, Br^-) ($p < 0.05$, $-0.71 \leq r_s \leq -0.39$), and $\delta^{18}O$ ($p<0.05$, $-0.38 \leq r_s \leq -0.37$). Furthermore, DNA concentrations negatively correlated with temperature ($p < 0.05$, $r_s = -0.37$) and pH ($p < 0.05$, $r_s = -0.44$), while TCC negatively correlated with temperature ($p < 0.01$, $r_s = -0.64$) and 16S rRNA gene copies with pH ($p < 0.01$, $r_s = -0.24$). Positive correlations were found for DNA and 16S rRNA gene copies with total organic carbon (TOC, $p < 0.05$, $r_s > 0.34$) and the water content ($p < 0.01$, $r_s = 0.47$).

3.3 Bacterial community composition

The most abundant bacterial taxa were Actinobacteria (class), Chloroflexi (Gitt-GS-136, KD4-96), Clostridia (class), Gemmatimonadetes, and Proteobacteria (primarily Alpha- and Betaproteobacteria) (Fig. 5). *Candidatus* Aminicenantes (candidate phylum OP8) and *Candidatus* Atribacteria (candidate phylum OP9) were highly abundant in core C3, where Actinobacteria, Chloroflexi, and Gemmatimonadetes were almost absent.

In order to test for correlation between the bacterial community composition at each drill site with environmental parameters like salinity and temperature, we performed Mantel tests (Table S11). We found no correlation with salinity, but a correlation to temperature ($p = 0.0001$, correlation $R = 0.25$). However, the community formation was stronger influenced by stable water isotopes ($p = 0.0001$, $R = 0.40$) and the sample depth ($p = 0.0001$, $R = 0.36$) in meters below sea floor (m bsf) and below surface (m bs), respectively, than by temperature.

We included those environmental parameters that showed a significant correlation with microbial community composition in a canonical correspondence analysis (CCA, Fig. 6). Accordingly, grouping patterns of the bacterial community based on the $OTU_{0.03}$ composition of the samples and the Bray-Curtis dissimilarity were visualized. The CCA showed a clustering of samples according to their borehole location for C2 and C3, while communities of C1 and C4 were more scattered. Samples located to the left side of the plot originated from a greater depth (C1 and C2) than samples to the right side (C3 and C4). Variance of samples from the bottom left to the top right was explained by rising temperature, while variance of samples from the top left to the bottom right are likely explained by decreasing values of the stable water isotopes $\delta^{18}O$ and δD. The bacterial community of C3 was most distinct and clustered furthest from communities of all other sites, and was linked with stable water isotopes and sample depth. The variance between C1, C4 and C2 samples are explained by temperature differences.

Despite the overlaps within the CCA ordination, a one-way PerMANOVA revealed that the variance between each of the clusters was significantly higher than within single clusters (Table S12), i.e., the bacterial subpopulations of each drill site were significantly different from each other.

4 Discussion

The present study aimed at understanding the effect of long-term permafrost warming independent of thaw on microbial community composition and abundance. The observed significant negative rank-based correlation between increasing temperature and total cell counts (TCC) contradicts our hypothesis that millennial-scale permafrost warming directly increases microbial abundance. It is, however, in line with related studies on arctic and subarctic soil microbial communities where a negative effect of increasing temperature on microbial abundance was assigned to freeze-thaw cycles (Schimel et al., 2007; Skogland et al., 1988) and substrate depletion (Walker et al., 2018). Both effects are, however, unlikely here. Firstly, sample depths were always more than 10 m below surface and sea floor, respectively, and freeze-thaw cycles within the investigated Unit II can be excluded. Secondly, preservation, rather than depletion, of substrates was more likely in the two submarine cores C3 and C4, where DOC contents were comparable to that of the cold terrestrial permafrost of C1 (Fig. S1). The degradation of DOC can be used as measure for microbial carbon turnover (Seto and Yanagiya, 1983) and the DOC

© Author(s) 2019. CC BY 4.0 License.

concentration usually correlates with microbial abundance (Junge et al., 2004; Smolander and Kitunen, 2002; Vetter et al., 2010). The cores C3 and C4 had significantly lower TCC and bacterial gene copy numbers than the onshore core C1 and the C2 core furthest offshore. Thus, microbial activity and substrate utilization were likely low in C3 and C4. A negative influence of permafrost warming on microbial abundance is further challenged through some indication for microbial proliferation in core C2, which had experienced longest warming of all cores. In detail, TCC in C2 were higher than in the other submarine cores while DOC values were significantly lower in C2 compared to all other cores (Dunn's test, Table S13). Permafrost warming for more than two millennia may have enabled microbial communities to adapt to the new temperature regime and sediment properties as suggested before (Mitzscherling et al., 2017). A direct effect of permafrost warming on microbial abundance was not evident; the effect of changing pore-water salinity is more plausible than that of permafrost warming. Rising salinity correlates significantly both with TCC and bacterial gene copy numbers. Also, TCC and bacterial 16S rRNA gene copy numbers were lowest in core C4, where pore-water salinities were elevated (electrical conductivity values >2000 µS cm^{-1}, Table S3). Low gene copy numbers may result from osmotic stress that limits microbial growth (Galinski, 1995; Rousk et al., 2011) and decreases microbial abundance in sediments (Jiang et al., 2007; Rath and Rousk, 2015; Rietz and Haynes, 2003; Wen et al., 2018). We argue that the different levels of salinity are relicts of the paleo-climate and varying landscape types (e.g. thermokarst lakes and lagoons, fluvial, floodplain, Fig. S4 and Table S14) that formed Unit II during the last glacial cycle, i.e. the Weichselian glaciation 117 – 10 ka BP (Svendsen et al., 2004). According to the IR-OSL ages Unit II of C4 was deposited ~60 ka BP and earlier. Conductivity values in C4 that were higher than 2000 µS cm^{-1} could be the result of strong evaporation. The climate in the Laptev Sea region during the middle Weichselian (75 – 25 ka BP) was of extremely continental type characterized by low precipitation throughout the year and relative warm summers (Hubberten et al., 2004). Also, salinity values in Unit II of core C4 are lower than in the seafloor sediments of the same core but higher than in the sediment layer in between (Fig. 2b), supporting the idea that differences in salinity reflect the paleo-environment and climate, and not an infiltration of seawater during the Holocene transgression. The presence of a temporary shallow thermokarst lake at the drilling site of C4 and following summer evaporation is one possible scenario leading to elevated salt concentrations (Larry Lopez et al., 2007). A strong influence of the paleo-climate on recent microbial abundance is further supported through a significant correlation between microbial abundance with $\delta^{18}O$ values (Table 1). The stable water isotope composition of ground ice is widely used as an archive for paleo-climatic information and for the determination of ground ice genesis (Meyer et al., 2002a, 2002b; Vasil'chuk, 1991). Compared to the other cores, C3 for example was enriched in heavy isotope species of $\delta^{18}O$ (-20 to -15‰) and δD (-150 to -160‰), suggesting warmer temperatures at the time of deposition (Meyer et al., 2002b). As ground ice is mainly fed by summer and winter precipitation, its isotopic composition reflects the annual range of air temperatures. Isotope changes towards heavier values could also be the result of larger amounts of summer rain as well as less winter snow preserved in the ice. Assuming that IR-OSL ages of Winterfeld et al. (2011) are correct, sediments of C3 were deposited at around 50 ka BP and later. Thus, C3 sediments were

© Author(s) 2019. CC BY 4.0 License.

probably deposited during a period where the extremely dry continental climate with relative warm summers was especially pronounced (between 45 and 35 ka BP) (Hubberten et al., 2004).

We suggest that microbial community composition like microbial abundance reflects the paleoclimate and sedimentation history and not a direct effect of permafrost warming. In detail, we observed a weak correlation between community composition with temperature and a strong correlation with stable water isotope values and depth, i.e. age. The microbial communities in core C3 which were most distinct from the other locations (Fig. 6) may thus reflect the higher paleo-temperatures and different proportions of summer and winter precipitation discussed earlier. Independent of core C3, microbial community composition showed substantial site specific differences. This local scale variation in community composition (β-diversity) likely results from the distance between the coring sites because β-diversity increases with increasing distance when environmental conditions differ (Lindström and Langenheder, 2012) and when dispersal is as limited as it is in permafrost environments (Bottos et al., 2018).

Irrespective of the effect of permafrost warming on microbial community composition and abundance, the cell counts and microbial taxa of this study expand our knowledge about microbial life in permafrost. The bacterial taxa dominating in the submarine permafrost samples were amongst the phyla that commonly occur in Artic permafrost and the active layer, like Proteobacteria, Firmicutes, Chloroflexi, Acidobacteria, Actinobacteria and Bacteroidetes (Jansson and Taş, 2014; Liebner et al., 2009; Mitzscherling et al., 2017; Taş et al., 2018). Furthermore, the most abundant taxa Actinobacteria, Chloroflexi, Firmicutes, Gemmatimonadetes and Proteobacteria (Fig. 5) are amongst the groups that were found to be active under frozen conditions in permafrost (Coolen and Orsi, 2015; Tuorto et al., 2014). The non-spore forming Actinobacteria were reported to dominate permafrost since they are well adapted to freezing conditions (Johnson et al., 2007). They are metabolically active at low temperatures and possess DNA-repair mechanisms. Firmicutes and Proteobacteria likely resist long-term exposure to subzero temperatures as they take advantage of nutrient and water availability (Johnson et al., 2007; Yergeau et al., 2010). In addition, many members of the Firmicutes are able to form spores. Atribacteria, which dominated in the core C3, were recently described to harbor functions for survival under extreme conditions like high salinities and cold temperatures (Glass et al., 2019).

The TCC of the onshore permafrost core C1 were in the upper range of cell counts (10^6-10^7 cells g^{-1}) reported for other permafrost environments (Gilichinsky et al., 2008; Jansson and Taş, 2014; Steven et al., 2006) and TCC of the three submarine permafrost cores were comparable to microbial abundances from organic carbon rich sub-seafloor sediments (10^5-10^7 cells g^{-1}) (Kallmeyer et al., 2012; Parkes et al., 2014). TCC and bacterial 16S rRNA gene abundance in cores C1 and C2, which were highest in this study, were at least one order of magnitude lower than values for the active layer, i.e. the seasonally thawed, upper permafrost layer (Kobabe et al., 2004; Liebner et al., 2008, 2015). This is in line with modelling studies on generation times in the subsurface where cells were reported to divide only every ten to hundred years (Jørgensen and Marshall, 2016; Starnawski et al., 2017). It also underlines that the effect of warming on microbial abundance in the investigated submarine permafrost cores was likely poor as discussed earlier. The observation that 16S rRNA gene copies

© Author(s) 2019. CC BY 4.0 License.

mostly exceeded TCC by an order of magnitude may reflect the long-term preservation of extracellular DNA due to low temperature conditions in permafrost (Stokstad, 2003; Willerslev et al., 2004) and, to a lesser extent, the appearance of multiple 16S rRNA gene copies per cell (Schmidt, 1998). Although qPCR is a good relative quantification method, it is only poorly related to cell counts (Lloyd et al., 2013). In addition, cell counts might be slightly underestimated due to hidden cells below sediment particles (Kallmeyer, 2011).

5 Conclusions

Substantial permafrost warming is occurring throughout the Arctic today and the associated response of microbial communities driving the biogeochemical cycling and the formation of greenhouse gases is of general interest. Inundation by seawater accelerates permafrost warming and results in a steady state of temperature under the present conditions within a few centuries. This makes submarine permafrost a suitable natural laboratory to study the microbial response on climate relevant time-scales. Our results demonstrate that both microbial abundance and community composition even after millennia of submarine permafrost warming by more than 10 °C reflect the paleo-climate and sedimentation history. However, even though we could not finally prove that long-term permafrost warming directly affects microbial abundance and bacterial community composition we found indications for it especially in the core that had experienced longest warming. This deserves more attention, because a direct effect of permafrost warming on microbial abundance, composition and carbon turnover would alter our understanding of the permafrost carbon feedback, which to date only considers permafrost thaw. Based on our work we suggest that future work addresses the responsiveness of microbial communities to permafrost warming through the analysis of organic matter quality (Fischer et al., 2002), chemical composition of permafrost DOM (Spencer et al., 2015; Sun et al., 1997; Ward and Cory, 2015), natural abundance isotope ratios of biomarkers (Boschker and Middelburg, 2002), metagenomics and metatranscriptomics (Coolen and Orsi, 2015; Mackelprang et al., 2017). Finally, in this study the length of the coring transect (~12 km), the age span within and between the cores and hence the comparatively long sedimentation period encompassed by our samples from Unit II had a stronger influence on recent microbial abundance and community than the large level of physicochemical similarity within this unit (Fig. 3 insert). Further studies on the microbial response to permafrost warming should focus on historically more similar samples without neglecting similar physicochemical properties.

Data availability

Sequences of the submarine permafrost communities presented in this work were deposited at the NCBI Sequence Read Archive (SRA) with the Project number BioProject ID# PRJNA352907. Bacterial 16S rRNA gene sequences have the sequence read archive accession numbers SRR7908003 - SRR7908028 and are available from Genbank, EMBL, and DDBJ.

© Author(s) 2019. CC BY 4.0 License.

(https://www.ncbi.nlm.nih.gov/bioproject/PRJNA352907, last access 15 January 2019) Environmental data of the sediment cores are available at https://doi.pangaea.de/10.1594/PANGAEA.895292.

Author contribution

SL, DW, MWk and JM formulated the research question and study design. PPO and MNG conducted field work. JM visualized the data and prepared graphs. MWf and PPO provided pore water and physicochemical data. FH conducted the bioinformatics analysis. LM performed and JK supported the cell counting. JM and SL prepared the original draft. All authors contributed to the discussion and interpretation of the data and the writing of the paper.

Competing Interest

The authors declare that they have no conflict of interest.

Acknowledgments

Our thanks go to Aleksandr Maslov (SB RAS, Melnikov Permafrost Institute, Yakutsk, Russia), who provided indispensable drilling expertise. We thank Tiksi Hydrobase staff members Viktor Bayderin, Viktor Dobrobaba, Sergey Kamarin, Valery Kulikov, Dmitry Mashkov, Dmitry Melnichenko, Aleksandr Safin, and Aleksandr Shiyan for their field support and Dimitry Yu. Bolshiyanov (Arctic Antarctic Research Institute, St. Petersburg) for logistical issues. Coring was supported by the German Ministry for Education and Research, a Joint Russian German Research Group (HGF-JRG100) of the Helmholtz Association of German Research Centres, and by the EU's INTAS program. Susanne Liebner is grateful for the funding of the Helmholtz Young Investigators Group (grant VH-NG-919). We further thank Anke Saborowski, Antje Eulenburg, Ute Bastian, and Katja Hockun for excellent laboratory support.

References

Allison, S. D., McGuire, K. L. and Treseder, K. K.: Resistance of microbial and soil properties to warming treatment seven years after boreal fire, Soil Biol. Biochem., 42(10), 1872–1878, doi:10.1016/j.soilbio.2010.07.011, 2010.

Anderson, M. J.: A new method for non parametric multivariate analysis of variance, Austral Ecol., 26, 32–46, doi:10.1111/j.1442-9993.2001.01070.pp.x, 2001.

Bischoff, J., Mangelsdorf, K., Gattinger, A., Schloter, M., Kurchatova, A. N., Herzschuh, U. and Wagner, D.: Response of methanogenic archaea to Late Pleistocene and Holocene climate changes in the Siberian Arctic, Global Biogeochem.

© Author(s) 2019. CC BY 4.0 License.

Cycles, 27(2), 305–317, doi:10.1029/2011GB004238, 2013.

Biskaborn, B. K., Smith, S. L., Noetzli, J., Matthes, H., Vieira, G., Streletskiy, D. A., Schoeneich, P., Romanovsky, V. E., Lewkowicz, A. G., Abramov, A., Allard, M., Boike, J., Cable, W. L., Christiansen, H. H., Delaloye, R., Diekmann, B., Drozdov, D., Etzelmüller, B., Grosse, G., Guglielmin, M., Ingeman-Nielsen, T., Isaksen, K., Ishikawa, M., Johansson, M., Johannsson, H., Joo, A., Kaverin, D., Kholodov, A., Konstantinov, P., Kröger, T., Lambiel, C., Lanckman, J.-P., Luo, D., Malkova, G., Meiklejohn, I., Moskalenko, N., Oliva, M., Phillips, M., Ramos, M., Sannel, A. B. K., Sergeev, D., Seybold, C., Skryabin, P., Vasiliev, A., Wu, Q., Yoshikawa, K., Zheleznyak, M. and Lantuit, H.: Permafrost is warming at a global scale, Nat. Commun., 10(1), 264, doi:10.1038/s41467-018-08240-4, 2019.

Boschker, H. T. S. and Middelburg, J. J.: Stable isotopes and biomarkers in microbial ecology, FEMS Microbiol. Ecol., 40(2), 85–95, doi:10.1111/j.1574-6941.2002.tb00940.x, 2002.

Boss, C. B. and Frieden, K. J.: Concepts, instrumentation, and techniques in inductively coupled plasma atomic emission spectrometry. Handbook Perkin-Elmer, Perkin- Elmer Corporation, USA., 1989.

Bottos, E. M., Kennedy, D. W., Romero, E. B., Fansler, S. J., Brown, J. M., Bramer, L. M., Chu, R. K., Tfaily, M. M., Jansson, J. K. and Stegen, J. C.: Dispersal limitation and thermodynamic constraints govern spatial structure of permafrost microbial communities, FEMS Microbiol. Ecol., 94, 1–48, doi:http://dx.doi.org/10.1101/265132, 2018.

Brown, J., Ferrians, Jr, O. J., Heginbottom, J. A. and Melnikov, E.: Circum-Arctic map of permafrost and ground-ice conditions, US Geological Survey, Washington DC., 1997.

Brown, J., Ferrians Jr., O. J., Heginbottom, J. A. and Melnikov, E. S.: Circum-Arctic Map of Permafrost and Ground-Ice Conditions, Version 2, Natl. Snow and Ice Data Cent., Boulder, Colo., 2002.

Coolen, M. J. L. and Orsi, W. D.: The transcriptional response of microbial communities in thawing Alaskan permafrost soils, Front. Microbiol., 6(197), 1–14, doi:10.3389/fmicb.2015.00197, 2015.

DeAngelis, K. M., Pold, G., Topçuoglu, B. D., van Diepen, L. T. a., Varney, R. M., Blanchard, J. L., Melillo, J. and Frey, S. D.: Long-term forest soil warming alters microbial communities in temperate forest soils, Front. Microbiol., 6(104), 1–13, doi:10.3389/fmicb.2015.00104, 2015.

Fischer, H., Wanner, S. C. and Pusch, M.: Bacterial abundance and production in river sediments as related to the biochemical composition of particulate organic matter (POM), Biogeochemistry, 61(1), 37–55, doi:10.1023/A:1020298907014, 2002.

Fritz, M., Vonk, J. E. and Lantuit, H.: Collapsing Arctic coastlines, Nat. Clim. Chang., 7(1), 6–7, doi:10.1038/nclimate3188, 2017.

Galinski, E. A.: Osmoadaptation in Bacteria, Adv. Microb. Physiol., 37, 273–328, doi:10.1016/S0065-2911(08)60148-4, 1995.

Gilichinsky, D., Vishnivetskaya, T., Petrova, M., Spirina, E., Mamykin, V. and Rivkina, E.: Bacteria in permafrost, in Psychrophiles: From Biodiversity to Biotechnology, edited by R. Margesin, pp. 83–102, Springer-Verlag, Berlin

© Author(s) 2019. CC BY 4.0 License.

Heidelberg., 2008.

Glass, J. B., Ranjan, P., Kretz, C. B., Nunn, B. L., Johnson, A. M., McManus, J. and Stewart, F. J.: Adaptations of Atribacteria to life in methane hydrates: hot traits for cold life, bioRxiv, 536078, doi:10.1101/536078, 2019.

Graham, D. E., Wallenstein, M. D., Vishnivetskaya, T. A., Waldrop, M. P., Phelps, T. J., Pfiffner, S. M., Onstott, T. C., Whyte, L. G., Rivkina, E. M., Gilichinsky, D. a, Elias, D. a, MacKelprang, R., Verberkmoes, N. C., Hettich, R. L., Wagner, D., Wullschleger, S. D. and Jansson, J. K.: Microbes in thawing permafrost: The unknown variable in the climate change equation, ISME J., 6(4), 709–712, doi:10.1038/ismej.2011.163, 2012.

Grigoriev, M. N.: Kriomorphogenez i litodinamika pribrezhno-shelfovoi zony morei Vostochnoi Sibiri (Cryomorphogenesis and lithodynamics of the East Siberian near-shore shelf zone), Russian Academy of Sciences, Siberian Branch [in Russian], Yakutsk., 2008.

Günther, F., Overduin, P. P., Sandakov, a. V., Grosse, G. and Grigoriev, M. N.: Short- and long-term thermo-erosion of ice-rich permafrost coasts in the Laptev Sea region, Biogeosciences, 10(6), 4297–4318, doi:10.5194/bg-10-4297-2013, 2013.

Hammer, Ø., Harper, D. A. T. and Ryan, P. D.: Paleontological Statistics Software: Package for Education and Data Analysis, Palaeontol. Electron., (4), 2001.

Hubberten, H. W., Andreev, A., Astakhov, V. I., Demidov, I., Dowdeswell, J. A., Henriksen, M., Hjort, C., Houmark-Nielsen, M., Jakobsson, M., Kuzmina, S., Larsen, E., Lunkka, J. P., Lyså, A., Mangerud, J., Möller, P., Saarnisto, M., Schirrmeister, L., Sher, A. V., Siegert, C., Siegert, M. J. and Svendsen, J. I.: The periglacial climate and environment in northern Eurasia during the Last Glaciation, Quat. Sci. Rev., 23(11–13), 1333–1357, doi:10.1016/j.quascirev.2003.12.012, 2004.

Hultman, J., Waldrop, M. P., Mackelprang, R., David, M. M., McFarland, J., Blazewicz, S. J., Harden, J., Turetsky, M. R., McGuire, A. D., Shah, M. B., VerBerkmoes, N. C., Lee, L. H., Mavrommatis, K. and Jansson, J. K.: Multi-omics of permafrost, active layer and thermokarst bog soil microbiomes, Nature, 521(7551), 208–212, doi:10.1038/nature14238, 2015.

IPCC in Climate Change 2013: The Physical Science Basis. Contribution of Working Group I to the Fifth Assessment Report of the Intergovernmental Panel on Climate Change, Cambridge Univ. Press, 1535, 2013.

Jansson, J. K. and Taş, N.: The microbial ecology of permafrost., Nat. Rev. Microbiol., 12(6), 414–425, doi:10.1038/nrmicro3262, 2014.

Jiang, H., Dong, H., Yu, B., Liu, X., Li, Y., Ji, S. and Zhang, C. L.: Microbial response to salinity change in Lake Chaka, a hypersaline lake on Tibetan plateau, Environ. Microbiol., 9(10), 2603–2621, doi:10.1111/j.1462-2920.2007.01377.x, 2007.

Johnson, S. S., Hebsgaard, M. B., Christensen, T. R., Mastepanov, M., Nielsen, R., Munch, K., Brand, T., Gilbert, M. T. P., Zuber, M. T., Bunce, M., Rønn, R., Gilichinsky, D., Froese, D. and Willerslev, E.: Ancient bacteria show evidence of

DNA repair, Proc. Natl. Acad. Sci., 104(36), 14401–14405, doi:10.1073/pnas.0706787104, 2007.

Jørgensen, B. B. and Marshall, I. P. G.: Slow Microbial Life in the Seabed, Ann. Rev. Mar. Sci., 8(1), 311–332, doi:10.1146/annurev-marine-010814-015535, 2016.

Junge, K., Eicken, H. and Deming, J. W.: Bacterial Activity at -2 to -20 degrees C in Arctic wintertime sea ice., Appl. Environ. Microbiol., 70(1), 550–557, doi:10.1128/AEM.70.1.550, 2004.

Junker, R., Grigoriev, M. N. and Kaul, N.: Non-contact infrared temperature measurements in dry permafrost boreholes, J. Geophys. Res. Soild Earth, 113(B4102), 1–10, doi:10.1029/2007JB004946, 2008.

Kallmeyer, J.: Detection and Quantification of Microbial Cells in Subsurface Sediments, 1st ed., Elsevier Inc., 2011.

Kallmeyer, J., Pockalny, R., Adhikari, R. R., Smith, D. C. and D'Hondt, S.: Global distribution of microbial abundance and biomass in subseafloor sediment, Proc. Natl. Acad. Sci., doi:10.1073/pnas.1203849109, 2012.

Kattsov, V. M., Källén, E., Cattle, H., Christensen, J., Drange, H., Hanssen-bauer, I., Jóhannesen, T., Karol, I., Räisänen, J., Svensson, G., Chen, D., Polyakov, I. and Rinke, A.: Future Climate Change: Modeling and Scenarios for the Arctic Lead Authors, in Arctic Climate Impact Assessment, pp. 99–150. [online] Available from: http://www.acia.uaf.edu/PDFs/ACIA_Science_Chapters_Final/ACIA_Ch04_Final.pdf, 2005.

Kneier, F., Overduin, P. P., Langer, M., Boike, J. and Grigoriev, M. N.: Borehole temperature reconstructions reveal differences in past surface temperature trends for the permafrost in the Laptev Sea region, Russian Arctic, arktos, 4(1), 7, doi:10.1007/s41063-018-0041-3, 2018.

Kobabe, S., Wagner, D. and Pfeiffer, E.-M.: Characterisation of microbial community composition of a Siberian tundra soil by fluorescence in situ hybridisation, FEMS Microbiol. Ecol., 50(1), 13–23, doi:10.1016/j.femsec.2004.05.003, 2004.

Koch, K., Knoblauch, C. and Wagner, D.: Methanogenic community composition and anaerobic carbon turnover in submarine permafrost sediments of the Siberian Laptev Sea, Environ. Microbiol., 11(3), 657–668, doi:10.1111/j.1462-2920.2008.01836.x, 2009.

Lantuit, H., Overduin, P. P., Couture, N., Wetterich, S., Aré, F., Atkinson, D., Brown, J., Cherkashov, G., Drozdov, D., Donald Forbes, L., Graves-Gaylord, A., Grigoriev, M., Hubberten, H. W., Jordan, J., Jorgenson, T., Ødegård, R. S., Ogorodov, S., Pollard, W. H., Rachold, V., Sedenko, S., Solomon, S., Steenhuisen, F., Streletskaya, I. and Vasiliev, A.: The Arctic Coastal Dynamics Database: A New Classification Scheme and Statistics on Arctic Permafrost Coastlines, Estuaries and Coasts, 35(2), 383–400, doi:10.1007/s12237-010-9362-6, 2012.

Larry Lopez, C. M., Brouchkov, A., Nakayama, H., Takakai, F., Fedorov, A. N. and Fukuda, M.: Epigenetic salt accumulation and water movement in the active layer of central Yakutia in eastern Siberia, Hydrol. Process., 21, 103–109, doi:10.1002/hyp, 2007.

Liebner, S., Harder, J. and Wagner, D.: Bacterial diversity and community structure in polygonal tundra soils from Samoylov Island, Lena Delta, Siberia, Int. Microbiol., 11(3), 195–202, doi:10.2436/20.1501.01.60, 2008.

Liebner, S., Rublack, K., Stuehrmann, T. and Wagner, D.: Diversity of aerobic methanotrophic bacteria in a permafrost active layer soil of the Lena Delta, Siberia, Microb. Ecol., 57(1), 25–35, doi:10.1007/s00248-008-9411-x, 2009.

Liebner, S., Ganzert, L., Kiss, A., Yang, S., Wagner, D. and Svenning, M. M.: Shifts in methanogenic community composition and methane fluxes along the degradation of discontinuous permafrost, Front. Microbiol., 6(356), 1–10, doi:10.3389/fmicb.2015.00356, 2015.

Lindström, E. S. and Langenheder, S.: Local and regional factors influencing bacterial community assembly, Environ. Microbiol. Rep., 4(1), 1–9, doi:10.1111/j.1758-2229.2011.00257.x, 2012.

Llobet-Brossa, E., Rossello-Mora, R. and Amann, R.: Microbial Community Composition of Wadden Sea Sediments as Revealed by Fluorescence In Situ Hybridization, Appl. Environ. Microbiol., 64(7), 2691–2696, 1998.

Lloyd, K. G., May, M. K., Kevorkian, R. T. and Steen, A. D.: Meta-analysis of quantification methods shows that archaea and bacteria have similar abundances in the subseafloor, Appl. Environ. Microbiol., 79(24), 7790–7799, doi:10.1128/AEM.02090-13, 2013.

Luo, C., Rodriguez-R, L. M., Johnston, E. R., Wu, L., Cheng, L., Xue, K., Tu, Q., Deng, Y., He, Z., Shi, J. Z., Yuan, M. M., Sherry, R. A., Li, D., Luo, Y., Schuur, E. A. G., Chain, P., Tiedje, J. M., Zhou, J. and Konstantinidis, K. T.: Soil microbial community responses to a decade of warming as revealed by comparative metagenomics., Appl. Environ. Microbiol., 80(5), 1777–86, doi:10.1128/AEM.03712-13, 2014.

Mackelprang, R., Waldrop, M. P., DeAngelis, K. M., David, M. M., Chavarria, K. L., Blazewicz, S. J., Rubin, E. M. and Jansson, J. K.: Metagenomic analysis of a permafrost microbial community reveals a rapid response to thaw, Nature, 480, 368–371, doi:10.1038/nature10576, 2011.

Mackelprang, R., Burkert, A., Haw, M., Mahendrarajah, T., Conaway, C. H., Douglas, T. a. and Waldrop, M. P.: Microbial survival strategies in ancient permafrost: Insights from metagenomics, ISME J., 11(10), 2305–2318, doi:10.1038/ismej.2017.93, 2017.

Mantel, N.: The Detection of Disease Clustering and a Generalized Regression Approach, Cancer Res., 27(1), 209–220, 1967.

Meyer, H., Schönicke, L., Wand, U., Hubberten, H. W. and Friedrichsen, H.: Isotope studies of hydrogen and oxygen in ground ice - Experiences with the equilibration technique, Isotopes Environ. Health Stud., 36(2), 133–149, doi:10.1080/10256010008032939, 2000.

Meyer, H., Dereviagin, A., Siegert, C., Schirrmeister, L. and Hubberten, H. W.: Palaeoclimate reconstruction on Big Lyakhovsky Island, North Siberia - Hydrogen and oxygen isotopes in ice wedges, Permafr. Periglac. Process., 13(2), 91–105, doi:10.1002/ppp.416, 2002a.

Meyer, H., Dereviagin, A., Siegert, C. and Hubberten, H.-W.: Paleoclimatic Studies on Bykovsky Peninsula, North Siberia - Hydrogen and Oxygen Isotopes in Ground Ice, Polarforschung, 70, 37–51, 2002b.

Mitzscherling, J., Winkel, M., Winterfeld, M., Horn, F., Yang, S., Grigoriev, M. N., Wagner, D., Overduin, P. P. and Liebner, S.: The development of permafrost bacterial communities under submarine conditions, J. Geophys. Res.

Biogeosciences, 122(7), 1689–1704, doi:10.1002/2017JG003859, 2017.

Overduin, P. P.: Russian-German Cooperation SYSTEM LAPTEV SEA: The expedition COAST I, in Expeditions in Siberia 2005, edited by L. Schirrmeister, pp. 1–40, Reports on Polar and Marine Research., 2007.

Overduin, P. P., Rachold, V. and Grigoriev, M. N.: The State of Subsea Permafrost in the Western Laptev Nearshore Zone, in Proceedings of the Ninth International Conference on Permafrost, Faribanks, Alaska, pp. 1345–1350., 2008.

Overduin, P. P., Liebner, S., Knoblauch, C., Günther, F., Wetterich, S., Schirrmeister, L., Hubberten, H. W. and Grigoriev, M. N.: Methane oxidation following submarine permafrost degradation: Measurements from a central Laptev Sea shelf borehole, J. Geophys. Res. G Biogeosciences, 120(5), 965–978, doi:10.1002/2014JG002862, 2015.

Parkes, R. J., Sass, H., Cragg, B. A., Webster, G., Roussel, E. G. P. and Weightman, A. J.: Studies on prokaryotic populations and processes in subseafloor sediments - an update, in Microbial Life of the Deep Biosphere, edited by J. Kallmeyer and D. Wagner, pp. 1–27, de Gruyter, Berlin., 2014.

Portnov, A., Smith, A. J., Mienert, J., Cherkashov, G., Rekant, P., Semenov, P., Serov, P. and Vanshtein, B.: Offshore permafrost decay and massive seabed methane escape in water depths >20 m at the South Kara Sea shelf, Geophys. Res. Lett., 40(15), 3962–3967, doi:10.1002/grl.50735, 2013.

Rachold, V., Bolshiyanov, D. Y., Grigoriev, M. N., Hubberten, H.-W., Junker, R., Kunitsky, V. V., Merker, F., Overduin, P. and Schneider, W.: Nearshore arctic subsea permafrost in transition, Eos, Trans. Am. Geophys. Union, 88(13), 149–150, doi:10.1029/2007EO130001, 2007.

Radujković, D., Verbruggen, E., Sigurdsson, B. D., Leblans, N. I. W., Janssens, I. A., Vicca, S. and Weedon, J. T.: Prolonged exposure does not increase soil microbial community compositional response to warming along geothermal gradients, FEMS Microbiol. Ecol., 94(2), 1–10, doi:10.1093/femsec/fix174, 2018.

Rath, K. M. and Rousk, J.: Salt effects on the soil microbial decomposer community and their role in organic carbon cycling : A review, Soil Biol. Biochem., 81, 108–123, doi:10.1016/j.soilbio.2014.11.001, 2015.

Rietz, D. N. and Haynes, R. J.: Effects of irrigation-induced salinity and sodicity on soil microbial activity, Soil Biol. Biochem., 35(6), 845–854, doi:10.1016/S0038-0717(03)00125-1, 2003.

Rinnan, R., Michelsen, A., Baath, E. and Jonasson, S.: Fifteen years of climate change manipulations alter soil microbial communities in a subarctic heath ecosystem, Glob. Chang. Biol., 13(1), 28–39, doi:DOI 10.1111/j.1365-2486.2006.01263.x, 2007.

Rivkina, E. M., Friedmann, E. I. and Mckay, C. P.: Metabolic Activity of Permafrost Bacteria below the Freezing Point, Appl. Environ. Microbiol., 66(8), 3230–3233, doi:10.1128/AEM.66.8.3230-3233.2000.Updated, 2000.

Romanovskii, N. N. and Hubberten, H. W.: Results of permafrost modelling of the lowlands and shelf of the Laptev Sea Region, Russia, Permafr. Periglac. Process., 12(2), 191–202, doi:10.1002/ppp.387, 2001.

Romanovskii, N. N., Hubberten, H. W., Gavrilov, A. V, Tumskoy, V. E. and Kholodov, A. L.: Permafrost of the east Siberian Arctic shelf and coastal lowlands, Quat. Sci. Rev., 23(11–13), 1359–1369,

© Author(s) 2019. CC BY 4.0 License.

doi:http://dx.doi.org/10.1016/j.quascirev.2003.12.014, 2004.

Romanovskii, N. N., Hubberten, H. W., Gavrilov, A. V., Eliseeva, A. A. and Tipenko, G. S.: Offshore permafrost and gas hydrate stability zone on the shelf of East Siberian Seas, Geo-Marine Lett., 25, 167–182, doi:10.1007/s00367-004-0198-6, 2005.

Rousk, J., Elyaagubi, F. K., Jones, D. L. and Godbold, D. L.: Bacterial salt tolerance is unrelated to soil salinity across an arid agroecosystem salinity gradient, Soil Biol. Biochem., 43(9), 1881–1887, doi:10.1016/j.soilbio.2011.05.007, 2011.

Rui, J., Li, J., Wang, S., An, J., Liu, W., Lin, Q., Yang, Y., He, Z. and Li, X.: Responses of Bacterial Communities to Simulated Climate Changes in Alpine Meadow Soil of the Qinghai-Tibet Plateau, Appl. Environ. Microbiol., 81(17), 6070–6077, doi:10.1128/AEM.00557-15, 2015.

Schimel, J., Balser, T. C. and Wallenstein, M.: Microbial Stress-Response Physiology and Its Implications for Ecosystem Function, Ecology, 88(6), 1386–1394, doi:10.1890/06-0219, 2007.

Schindlbacher, A., Rodler, A., Kuffner, M., Kitzler, B., Sessitsch, A. and Zechmeister-Boltenstern, S.: Experimental warming effects on the microbial community of a temperate mountain forest soil, Soil Biol. Biochem., 43(7), 1417–1425, doi:10.1016/j.soilbio.2011.03.005, 2011.

Schmidt, T. M.: Multiplicity of Ribosomal RNA Operons in Prokaryotic Genomes, in Bacterial Genomes, pp. 221–229, Springer US, Boston, MA., 1998.

Schuur, E. A. G., Bockheim, J., Canadell, J. G., Euskirchen, E., Field, C. B., Goryachkin, S. V, Hagemann, S., Kuhry, P., Lafleur, P. M., Lee, H., Mazhitova, G., Nelson, F. E., Rinke, A., Romanovsky, V. E., Shiklomanov, N., Tarnocai, C., Venevsky, S., Vogel, J. G. and Zimov, S. A.: Vulnerability of permafrost carbon to climate change: Implications for the global carbon cycle, Bioscience, 58(8), 701–714, doi:10.1641/B580807, 2008.

Schuur, E. A. G., Vogel, J. G., Crummer, K. G., Lee, H., Sickman, J. O. and Osterkamp, T. E.: The effect of permafrost thaw on old carbon release and net carbon exchange from tundra, Nature, 459, 556–559, doi:10.1038/Nature08031, 2009.

Seto, M. and Yanagiya, K.: Rate of CO2 evolution from soil in relation to temperature and amount of dissolved organic carbon, Japanese J. Ecol., 33, 199–205, 1983.

Shakhova, N., Semiletov, I., Salyuk, A., Yusupov, V., Kosmach, D. and Gustafsson, Ö.: Extensive Methane Venting to the Atmosphere from Sediments of the East Siberian Arctic Shelf, Science (80-.)., 327, 1246–1250, doi:10.1126/science.1229223, 2010.

Shakhova, N., Semiletov, I., Leifer, I., Sergienko, V., Salyuk, A., Kosmach, D., Chernykh, D., Stubbs, C., Nicolsky, D., Tumskoy, V. and Gustafsson, Ö.: Ebullition and storm-induced methane release from the East Siberian Arctic Shelf, Nat. Geosci., 7, 64–70, doi:10.1038/ngeo2007, 2014.

Skogland, T., Lomeland, S. and Goksøyr, J.: Respiratory burst after freezing and thawing of soil: Experiments with soil bacteria, Soil Biol. Biochem., 20(6), 851–856, doi:10.1016/0038-0717(88)90092-2, 1988.

Smolander, A. and Kitunen, V.: Soil microbial activities and characteristics of dissolved organic C and N in relation to tree species, Soil Biol. Biochem., 34, 651–660, doi:10.1016/S0038-0717(01)00227-9, 2002.

Spencer, R. G. M., Mann, P. J., Dittmar, T., Eglinton, T. I., McIntyre, C., Holmes, R. M., Zimoc, N. and Stubbins, A.: Detecting the signature of permafrost thaw in Arctic rivers, Geophys. Res. Lett., 42(8), 1–6, doi:https://doi.org/10.1002/2015GL063498, 2015.

Starnawski, P., Bataillon, T., Ettema, T. J. G., Jochum, L. M., Schreiber, L., Chen, X., Lever, M. a., Polz, M. F., Jørgensen, B. B., Schramm, A. and Kjeldsen, K. U.: Microbial community assembly and evolution in subseafloor sediment, Proc. Natl. Acad. Sci., 114(11), 2940–2945, doi:10.1073/pnas.1614190114, 2017.

Steven, B., Léveillé, R., Pollard, W. H. and Whyte, L. G.: Microbial ecology and biodiversity in permafrost, Extremophiles, 10(4), 259–267, doi:10.1007/s00792-006-0506-3, 2006.

Stokstad, E.: Ancient DNA Pulled From Soil, Science (80-.)., 300(5618), 407a–407, doi:10.1126/science.300.5618.407a, 2003.

Sun, L., Perdue, E. M., Meyer, J. L. and Weis, J.: Use of elemental composition to predict bioavailability of dissolved organic matter in a Georgia river, Limnol. Oceanogr., 42(4), 714–721, doi:10.4319/lo.1997.42.4.0714, 1997.

Svendsen, J. I., Alexanderson, H., Astakhov, V. I., Demidov, I., Dowdeswell, J. a., Funder, S., Gataullin, V., Henriksen, M., Hjort, C., Houmark-Nielsen, M., Hubberten, H. W., Ingólfsson, Ó., Jakobsson, M., Kjær, K. H., Larsen, E., Lokrantz, H., Lunkka, J. P., Lyså, A., Mangerud, J., Matiouchkov, A., Murray, A., Möller, P., Niessen, F., Nikolskaya, O., Polyak, L., Saarnisto, M., Siegert, C., Siegert, M. J., Spielhagen, R. F. and Stein, R.: Late Quaternary ice sheet history of northern Eurasia, Quat. Sci. Rev., 23(11–13), 1229–1271, doi:10.1016/j.quascirev.2003.12.008, 2004.

Tarnocai, C., Canadell, J. G., Schuur, E. A. G., Kuhry, P., Mazhitova, G. and Zimov, S.: Soil organic carbon pools in the northern circumpolar permafrost region, Global Biogeochem. Cycles, 23(2), GB2023, doi:10.1029/2008gb003327, 2009.

Taş, N., Prestat, E., Wang, S., Wu, Y., Ulrich, C., Kneafsey, T., Tringe, S. G., Torn, M. S., Hubbard, S. S. and Jansson, J. K.: Landscape topography structures the soil microbiome in arctic polygonal tundra, Nat. Commun., 9(1), doi:10.1038/s41467-018-03089-z, 2018.

Taylor, J. P., Wilson, B., Mills, M. S. and Burns, R. G.: Comparison of microbial numbers and enzymatic activities in surface soils and subsoils using various techniques, Soil Biol. Biochem., 34(3), 387–401, doi:10.1016/S0038-0717(01)00199-7, 2002.

Thornton, B. F., Geibel, M. C., Crill, P. M., Humborg, C. and Mörth, C. M.: Methane fluxes from the sea to the atmosphere across the Siberian shelf seas, Geophys. Res. Lett., 43(11), 5869–5877, doi:10.1002/2016GL068977, 2016.

Tuorto, S. J., Darias, P., Mcguinness, L. R., Panikov, N., Zhang, T., Häggblom, M. M. and Kerhof, L. J.: Bacterial genome replication at subzero temperatures in permafrost, ISME J., 8, 139–149, doi:10.1038/ismej.2013.140, 2014.

Vasil'chuk, Y. K.: Reconstruction of the paleoclimate of the Late Pleistocene and Holocene of the basis of isotope studies of subsurface ice and waters of the permafrost zone, Water Resour., 17(6), 640–647, 1991.

© Author(s) 2019. CC BY 4.0 License.

Vetter, A., Vieth, A., Mangelsdorf, K., Lerm, S., Alawi, M., Wolfgramm, M., Seibt, A. and Wurdemann, H.: Biogeochemical Characterisation of Geothermally Used Groundwater in Germany, in Proceedings World Geothermal Congress, pp. 1–6, Bali., 2010.

Wagner, D., Gattinger, A., Embacher, A., Pfeiffer, E.-M., Schloter, M. and Lipski, A.: Methanogenic activity and biomass in Holocene permafrost deposits of the Lena Delta, Siberian Arctic and its implication for the global methane budget, Glob. Chang. Biol., 13(5), 1089–1099, doi:10.1111/j.1365-2486.2007.01331.x, 2007.

Waldrop, M. P., Wickland, K. P., White, R., Berhe, a. a., Harden, J. W. and Romanovsky, V. E.: Molecular investigations into a globally important carbon pool: Permafrost-protected carbon in Alaskan soils, Glob. Chang. Biol., 16(9), 2543–2554, doi:10.1111/j.1365-2486.2009.02141.x, 2010.

Walker, T. W. N., Kaiser, C., Strasser, F., Herbold, C. W., Leblans, N. I. W., Woebken, D., Janssens, I. a., Sigurdsson, B. D. and Richter, A.: Microbial temperature sensitivity and biomass change explain soil carbon loss with warming, Nat. Clim. Chang., 8, 885–889, doi:10.1038/s41558-018-0259-x, 2018.

Ward, C. P. and Cory, R. M.: Chemical composition of dissolved organic matter draining permafrost soils, Geochim. Cosmochim. Acta, 167, 63–79, doi:10.1016/j.gca.2015.07.001, 2015.

Watanabe, K. and Mizoguchi, M.: Amount of unfrozen water in frozen porous media saturated with solution, Cold Reg. Sci. Technol., 34(2), 103–110, doi:10.1016/S0165-232X(01)00063-5, 2002.

Weedon, J. T., Kowalchuk, G. A., Aerts, R., van Hal, J., van Logtestijn, R., Taş, N., Röling, W. F. M. and van Bodegom, P. M.: Summer warming accelerates sub-arctic peatland nitrogen cycling without changing enzyme pools or microbial community structure, Glob. Chang. Biol., 18(1), 138–150, doi:10.1111/j.1365-2486.2011.02548.x, 2012.

Weedon, J. T., Kowalchuk, G. A., Aerts, R., Freriks, S., Röling, W. F. M. and van Bodegom, P. M.: Compositional stability of the bacterial community in a climate-sensitive Sub-Arctic Peatland, Front. Microbiol., 8(317), 1–11, doi:10.3389/fmicb.2017.00317, 2017.

Wegner, C., Hölemann, J. A., Dmitrenko, I., Kirillov, S. and Kassens, H.: Seasonal variations in Arctic sediment dynamics - Evidence from 1-year records in the Laptev Sea (Siberian Arctic), Glob. Planet. Change, 48, 126–140, doi:10.1016/j.gloplacha.2004.12.009, 2005.

Weiss, J.: Ionenchromatographie, 3rd ed., Wiley-VHC, Weinheim., 2001.

Wen, X., Unger, V., Jurasinski, G., Koebsch, F., Horn, F., Rehder, G., Sachs, T., Zak, D., Lischeid, G., Knorr, K.-H., Böttcher, M. E., Winkel, M., Bodeller, P. L. E. and Liebner, S.: Predominance of methanogens over methanotrophs contributes to high methane emissions in rewetted fens, Biogeosciences Discuss., 15(21), 6519–6536, doi:10.5194/bg-2018-184, 2018.

Willerslev, E., Hansen, A. J., Rønn, R., Brand, T. B., Barnes, I., Wiuf, C., Gilichinsky, D., Mitchell, D. and Cooper, A.: Long-term persistence of bacterial DNA, Curr. Biol., 14(1), 13–14, doi:10.1016/j.cub.2003.12.012, 2004.

Winkel, M., Mitzscherling, J., Overduin, P. P., Horn, F., Winterfeld, M., Rijkers, R., Grigoriev, M. N., Knoblauch, C., Mangelsdorf, K., Wagner, D. and Liebner, S.: Anaerobic methanotrophic communities thrive in deep submarine permafrost, Sci. Rep., 8(1), 1–13, doi:10.1038/s41598-018-19505-9, 2018.

Winterfeld, M., Schirrmeister, L., Grigoriev, M. N., Kunitsky, V. V., Andreev, A., Murray, A. and Overduin, P. P.: Coastal permafrost landscape development since the Late Pleistocene in the western Laptev Sea, Siberia, Boreas, 40(4), 697–713, doi:10.1111/j.1502-3885.2011.00203.x, 2011.

Xiong, J., Sun, H., Peng, F., Zhang, H., Xue, X., Gibbons, S. M., Gilbert, J. a. and Chu, H.: Characterizing changes in soil bacterial community structure in response to short-term warming, FEMS Microbiol. Ecol., 89(2), 281–292, doi:10.1111/1574-6941.12289, 2014.

Xu, G., Chen, J., Berninger, F., Pumpanen, J., Bai, J., Yu, L. and Duan, B.: Labile, recalcitrant, microbial carbon and nitrogen and the microbial community composition at two Abies faxoniana forest elevations under elevated temperatures, Soil Biol. Biochem., 91, 1–13, doi:10.1016/J.SOILBIO.2015.08.016, 2015.

Yergeau, E., Hogues, H., Whyte, L. G. and Greer, C. W.: The functional potential of high Arctic permafrost revealed by metagenomic sequencing, qPCR and microarray analyses, ISME J., 4(9), 1206–1214, doi:10.1038/ismej.2010.41, 2010.

Zhang, K., Shi, Y., Jing, X., He, J. S., Sun, R., Yang, Y., Shade, A. and Chu, H.: Effects of short-term warming and altered precipitation on soil microbial communities in alpine grassland of the tibetan plateau, Front. Microbiol., 7(1032), 1–11, doi:10.3389/fmicb.2016.01032, 2016.

Zhang, T., Barry, R. G., Knowles, K., Ling, F. and Armstrong, R. L.: Distribution of seasonally and perennially frozen ground in the Northern Hemisphere, in Proceedings of the 8th International Conference on Permafrost, edited by A. Phillips, Springman, pp. 1289–1294, Permafrost, Zürich., 2003.

Zhang, W., Parker, K. M., Luo, Y., Wan, S., Wallace, L. L. and Hu, S.: Soil microbial responses to experimental warming and clipping in a tallgrass prairie, Glob. Chang. Biol., 11(2), 266–277, doi:10.1111/j.1365-2486.2005.00902.x, 2005.

Zhou, J., Bruns, M. A. and Tiedje, J. M.: DNA recovery from soils of diverse composition, Appl. Environ. Microbiol., 62(2), 316–322, 1996.

Zimov, S. A., Schuur, E. A. and Chapin 3rd, F. S.: Permafrost and the global carbon budget, Science (80-.)., 312(5780), 1612–1613, doi:10.1126/science.1128908, 2006.

Zogg, G. P., Zak, D. R., Ringelberg, D. B., White, D. C., MacDonald, N. W. and Pregitzer, K. S.: Compositional and Functional Shifts in Microbial Communities Due to Soil Warming, Soil Sci. Soc. Am. J., 61(2), 475, doi:10.2136/sssaj1997.03615995006100020015x, 1997.

Biogeosciences Discuss., https://doi.org/10.5194/bg-2019-144
Manuscript under review for journal Biogeosciences
Discussion started: 6 May 2019
© Author(s) 2019. CC BY 4.0 License.

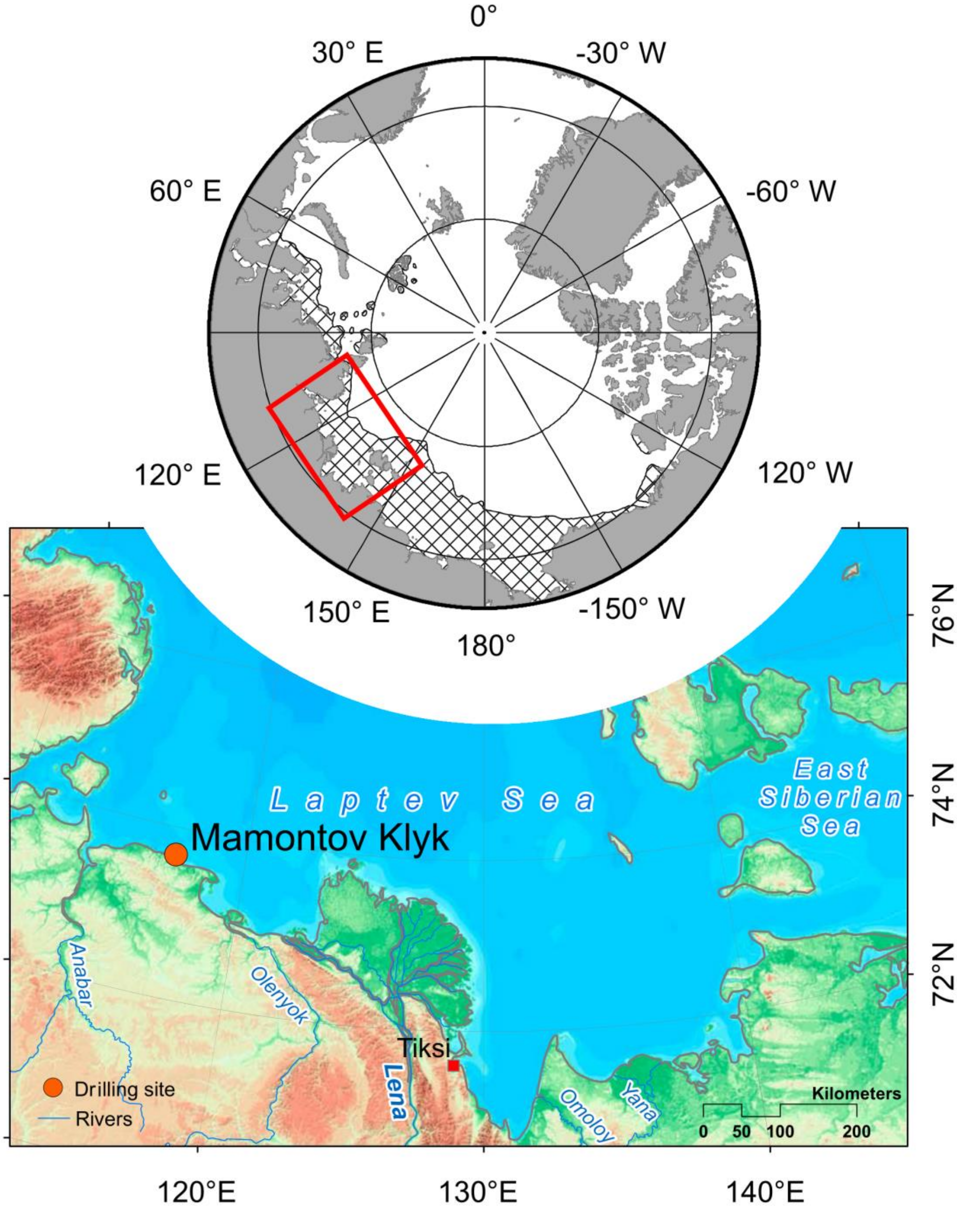

Figure 1: Geographical location of the study site. Location of the Laptev Sea on a circumpolar perspective map and the potential extent of submarine permafrost (striped area, based on (Brown et al., 2002)), as well as the geographical location of the drilling site at Cape Mamontov Klyk in the western Laptev Sea. (modified from (Overduin et al., 2015)).

© Author(s) 2019. CC BY 4.0 License.

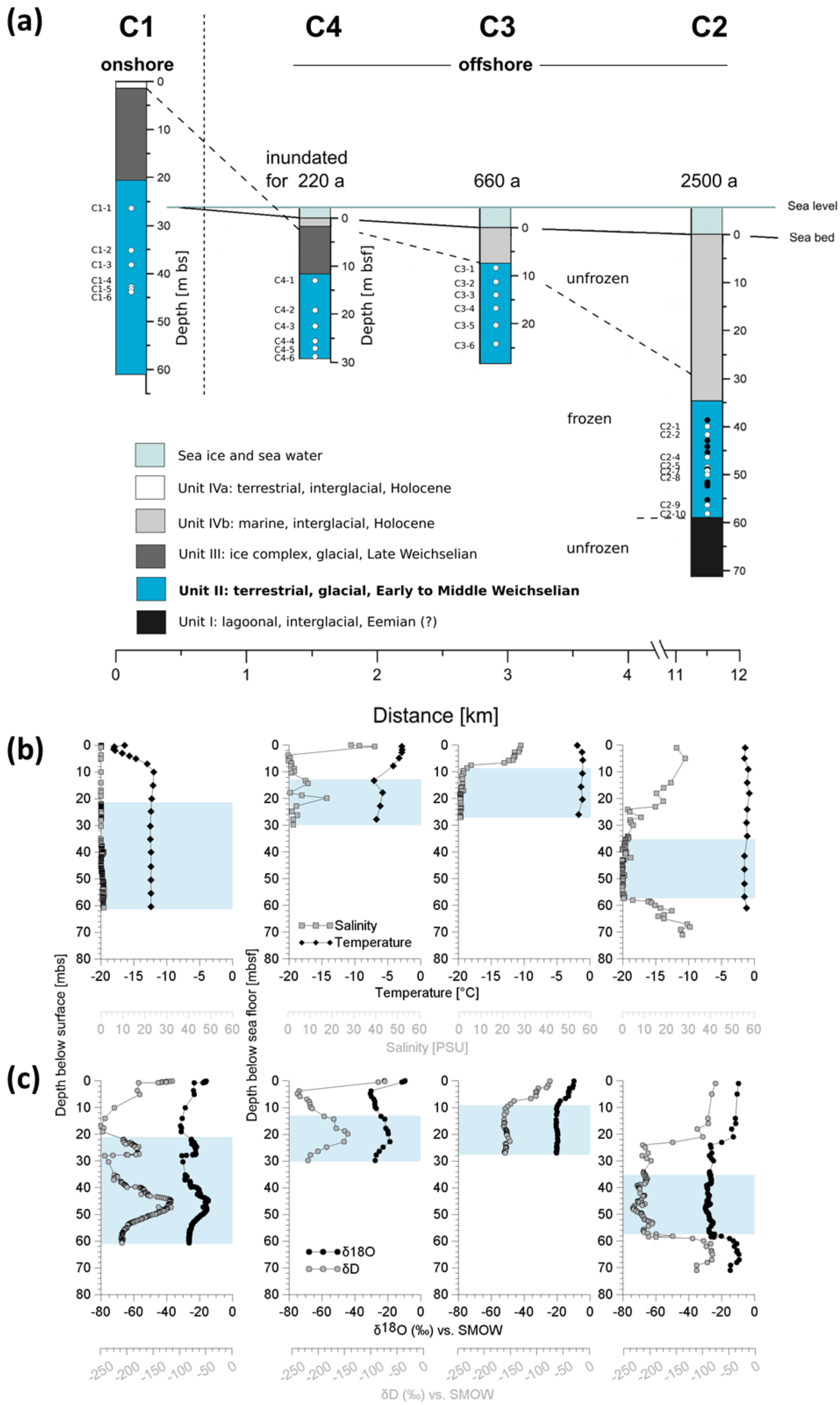

© Author(s) 2019. CC BY 4.0 License.

Figure 2: Overview of the coring transect, position and characteristics of the terrestrial and the submarine sediment cores. a) Periods of inundation are indicated above each submarine core. Core depth of the terrestrial core is given in m below surface (m bs) and depth of the submarine cores in meters below sea floor (m bsf). The core depths are proportional to each other, whereas the distance scale is only schematic. Affiliation of sediment deposits to discrete sediment units (Unit I - IVb), accumulated under similar environmental conditions in the same glacial or interglacial period, are distinguished by colours. Dots show the depth of the molecular samples. White dots represent samples from this study. Their denomination is indicated to the left. Black dots represent samples from a previous study. **b)** Depth profiles of temperature (black diamonds) and salinity (grey squares) as well as of **c)** the stable water isotopes δ^{18}O (black circles) and δD (grey circles) from the cores C1, C4, C3 and C2. The blue shaded area represents Unit II.

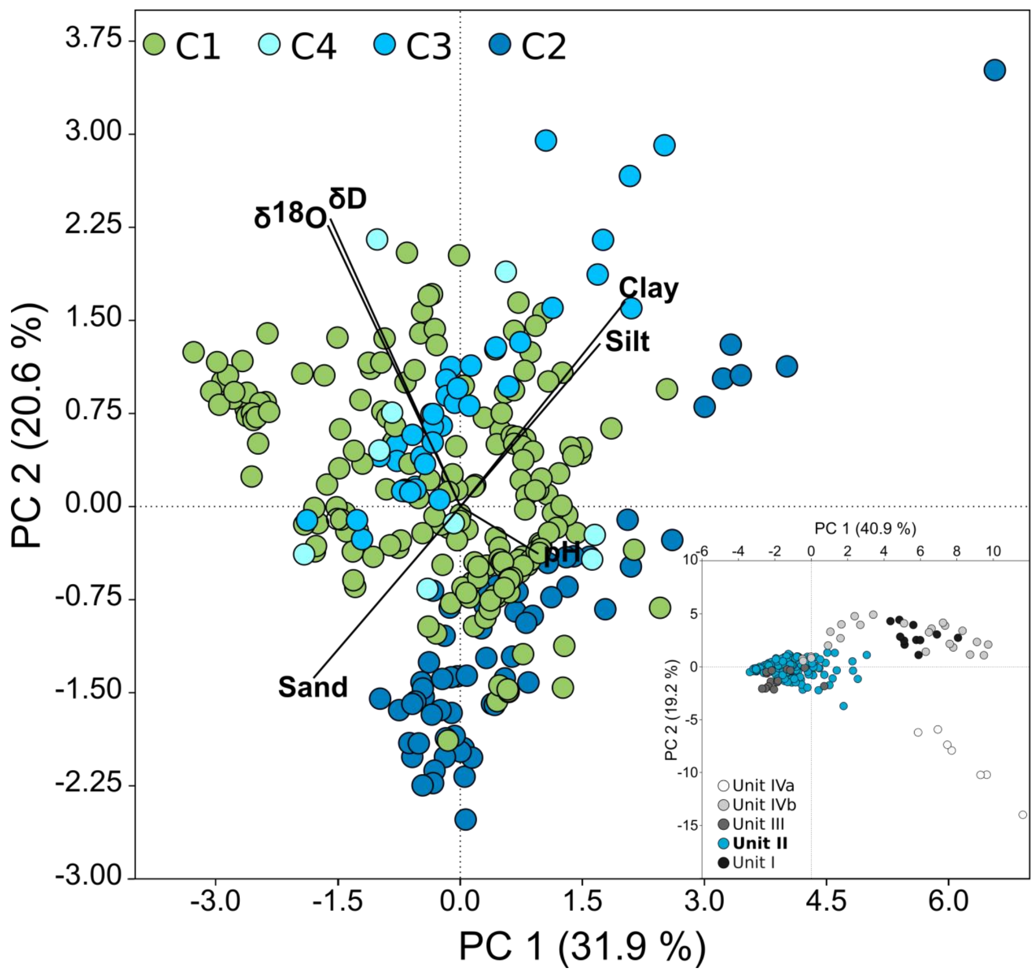

Figure 3: PCA of environmental, sedimentological and pore water data from Unit II of all four cores with PC 1 explaining 31.9% and PC 2 explaining 20.6 % of the variance between samples. Vectors show selected physicochemical factors that are mainly responsible for the variance between samples (see loadings plot Fig. S3). C1: n = 183, C2: n = 66, C3: n = 38, C4: n = 9. Outliers located outside the 95% ellipses were removed. The **insert** presents all samples of the onshore-offshore transect coloured irrespective of the cores by Unit (n = 361).

Biogeosciences Discuss., https://doi.org/10.5194/bg-2019-144
Manuscript under review for journal Biogeosciences
Discussion started: 6 May 2019
© Author(s) 2019. CC BY 4.0 License.

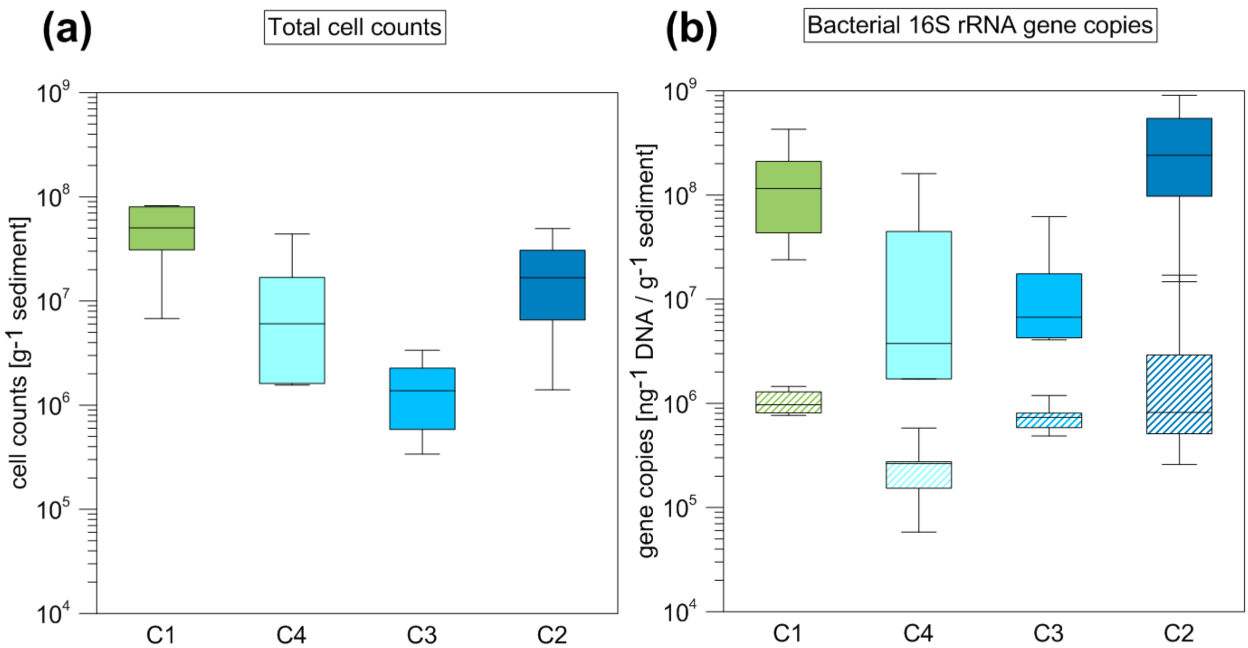

Figure 4: Boxplots of microbial and bacterial abundance in Unit II. a) Total cell counts and **b)** bacterial 16S rRNA gene copy numbers normalized to gram sediment wet weight (top, solid boxes) and to DNA concentration in ng (bottom, striped boxes) of the cores C1, C4, C3 and C2. Box plots contain the mean values obtained from two technical replicates of cell counts and three technical replicates of 16S rRNA gene copy numbers per biological replicate. Median lines are indicated within the boxes of which the size corresponds to ± 25% of the data, whereas the whiskers show the minimum and maximum of all data. Minimum, maximum and mean values, as well as standard deviation and sample numbers can be found in Table S9.

© Author(s) 2019. CC BY 4.0 License.

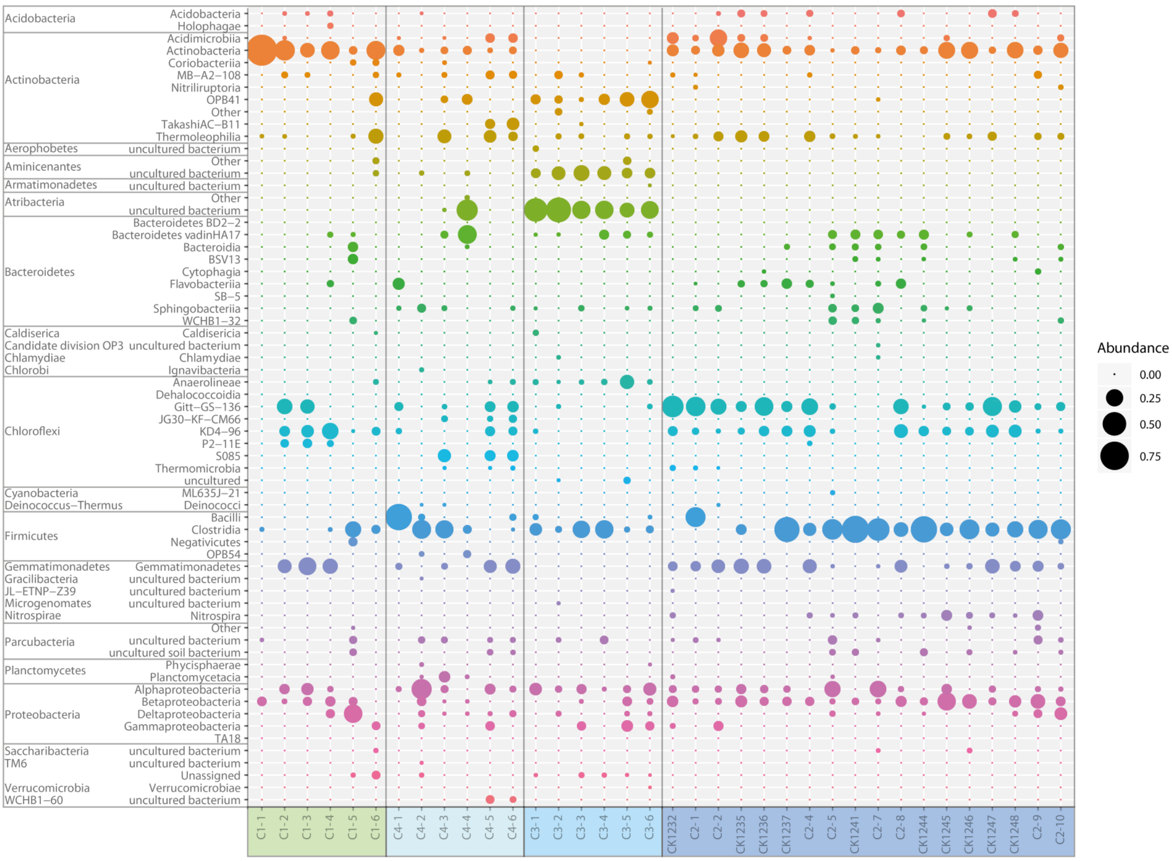

Figure 5: Relative abundance of bacterial classes from Unit II of the C1 - C4 cores. Coloured boxes and sample names below indicate the particular core. Sample names were explained earlier. Bubbles represent the mean value of relative abundances from two technical replicates.

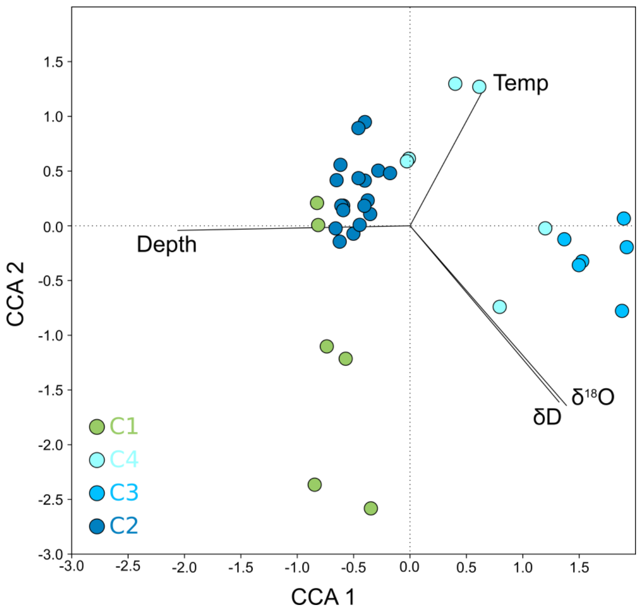

Figure 6: Canonical correspondence analysis (CCA) of $OTU_{0.03}$ data from Unit II in dependence on the environmental parameters temperature (Temp), sample depth (Depth) and the stable water isotopes $\delta^{18}O$ and δD. Each dot represents the mean value of relative OTU abundances from two technical replicates. Sample depth is denoted as meters below the surface for terrestrial samples and meters below the sea floor for submarine samples.

© Author(s) 2019. CC BY 4.0 License.

	Temp	Salinity	Depth [mbs/ mbsf]	Ba^{2+}	K^{+}	Mg^{2+}	Na^{+}	Cl^{-}	Br^{-}	$\delta^{18}O$	δD	pH	TC	TOC	Grav. Water Content
DNA	**-0.37**	**-0.35**	0.30	-0.08	**-0.39**	-0.32	**-0.39**	**-0.43**	**-0.41**	**-0.37**	-0.33	**-0.44**	**0.40**	**0.34**	**0.47**
16S rRNA Bacteria	-0.24	**-0.48**	**0.51**	0.03	**-0.49**	**-0.46**	**-0.57**	**-0.56**	**-0.54**	**-0.38**	-0.33	**-0.52**	**0.44**	**0.39**	**0.47**
TCC	**-0.64**	**-0.44**	0.26	**-0.38**	**-0.42**	**-0.37**	**-0.50**	**-0.52**	**-0.50**	**-0.37**	**-0.37**	-0.28	0.06	0.14	0.16

Table 1: Spearman correlations of DNA concentration, 16S rRNA gene copy numbers (g^{-1} sediment) and total cell counts (TCC) with environmental and geochemical parameters. Presented is the correlation coefficient r_s. Significant negative correlations are highlighted in red and significant positive correlations are highlighted in green. Colour intensity represents the significance levels, from dark to light colour: $p < 0.001$; $p < 0.01$; $p < 0.05$. P-values and more data can be found in Table S10.